

The effect of redshift function on the Weak Energy Conditions in $f(R)$ Wormholes

Amid Sadeghi Nezhad¹
Mohammad Reza Mehdizadeh²
Hanif Golchin³

*Faculty of Physics, Shahid Bahonar University of Kerman,
PO Box 76175, Kerman, Iran and*

Abstract

In the present paper, we investigate traversable wormhole solutions determined by an exponential shape function and fractional redshift function in the background of four viable $f(R)$ models. Although in the absence of the redshift function $\varphi(r)$ the null energy condition (NEC) and weak energy condition (WEC) are violated, we find that considering the redshift function, NEC and WEC are respected by choosing the appropriate parameters in the models. We also investigate the conditions of stability and absence of anti-gravity effects for these wormholes. Our results show that in the case of $\varphi(r) \neq 0$ these conditions are satisfied easier than the case of $\varphi(r) = 0$. Finally we calculate the deflection angle using the gravitational lensing effect. We show that the deflection angle increases by inserting the redshift function.

¹amidsadeghinezhad@phy.uk.ac.ir

²mehdizadeh.mr@uk.ac.ir

³h.golchin@uk.ac.ir

Contents

1	Introduction	1
2	Field equations and wormhole geometry in $f(R)$ gravity	3
3	Traversable wormhole solutions in $f(R)$ models	6
3.1	Case <i>I</i> : The Exponential gravity model	9
3.2	Case <i>II</i> : The tsujikawa model	11
3.3	Case <i>III</i> : The Starobisky gravity model	13
3.4	Case <i>IV</i> : The Hu-Sawicki model	16
4	Gravitational lensing and Particle Trajectories Around the Wormhole	18
4.1	Effective Potential	19
4.2	The Deflection Angle	21
5	Conclusions	22

1 Introduction

Wormholes are assumptive topological tunnels which connect two different space-times of the same universe, or even two separate universes by a minimal surface called the "throat" of the wormhole. Concept of inter-universe connections can be traced back to 1916 through the pioneering work of Flamm [1], shortly after the inception of General Relativity. In 1935, Einstein and Rosen developed a bridge model [2] by using the Flamms theories. The notion of a "wormhole" as a concise topological pathway in the space-time was initially postulated by Misner and Wheeler [3]. In 1988, Lorentzian wormholes, which provide the possibility of bidirectional transit of matter and energy, were initially explored by Morris and Thorne [4] in the framework of Einstein's theory of general relativity.

To assure the dual-directional traversability of the wormhole, the throat's geometry should satisfy the flaring-out condition [3]. This condition ensures that the throat expands as one moves away from its center, preventing collapse and allowing for bidirectional transit of matter and information. In four-dimensional general relativity, the flaring-out condition

leads to the violation of NEC and WEC. This necessitate the presence of "exotic matter" in the structure of the wormhole throat, characterized by a negative energy density [5]. Despite the fact that exotic matter has not been found in the physical world, efforts are being made to search for evidence of its existence in the cosmos [6]. There are some investigations with the aim of eliminating or minimizing the use of exotic matter in wormholes construction, by applying of the modified theories of gravity [7]. Modified gravity theories are alternative approaches to rectify the deficiencies or limitations in Einstein's general relativity. In recent years, large number of modified gravity models are investigated in the field of gravity and cosmology [8]. These innovative theories present additional terms to modify the field equations, or to change the geometric structure of the space-time which provide explanations for the physical and cosmological phenomena. For instance, by introducing higher-order terms in curvature, it becomes possible to create thin-shell wormholes that are created by standard matter [9].

Recently, through the application of modified gravity theories, broad exploration has been done to construct the wormhole configurations that do not rely on exotic matter [10]. In 2007, an investigation of thin-shell wormholes in the context of Einstein-Gauss-Bonnet gravity was carried out [11]. In 2011, descriptions regarding the energy flux emitted onto wormholes in Brans-Dicke theory were provided for Observational Manifestations [12]. Properties and existence of the wormhole throats in $f(R)$ gravity is explored in [13]. Wormhole geometries in the framework of third-order Love-lock gravity is also studied in 2016 [14]. In 2016 Lorentzian wormhole solutions are obtained in scalar-tensor gravity [15] and charged wormhole solutions satisfying NEC and WEC, are derived in Einstein-Cartan gravity [16] in 2019. In the framework of cubic gravity, the wormhole solutions that respect the energy conditions at the throat, are found in [17].

One of the most widely used modifications to General Relativity is the $f(R)$ gravity which was proposed by Buchadahl [18] in 1977. In $f(R)$ gravity, the curvature scalar or Ricci scalar R in the Einstein-Hilbert action is replaced by $f(R)$, which represents an arbitrary function of the Ricci scalar R . This modification leads to a generalized form of the Einstein field equations in this theory [19]. Indeed, these generalized equations have demonstrated hopeful descriptions of cosmic phenomena. In 2011, the hydrostatic equilibrium of stellar structure was studied in the context of the modified $f(R)$ gravity [20]. Neutron stars in $f(R)$ gravity were investigated in 2016 [21]. An analysis of extended stellar kinematics of elliptical galaxies considering the modified $f(R)$ gravity was provided in 2012 [22]. The gravitational interactions of galaxy clusters were described in 2014, utilizing $f(R)$ gravity [23]. The structure formation and evolution of the universe are also investigated by considering the

$f(R)$ gravity effects [24, 25, 26, 27]. Traversable wormhole geometries satisfying the energy conditions were achieved by Lobo and Oliveira in 2009 [28]. Lorentzian wormhole solutions were explored by Pavlovica and Sossich in 2015, satisfy the WEC [19]. A class of thin-shell wormhole solutions in the context of $f(R)$ gravity was constructed in 2016 [29]. Several viable $f(R)$ models were investigated in 2019 to derive wormhole solutions that satisfy the criteria of the NEC and WEC [30]. Another class of wormhole solutions has been investigated in studies [31] [32] through the selection of the shape function and redshift function. Bronnikov et al also discussed the wormhole non-existence conditions in the context of $f(R)$ theories [33].

In this research, our target is to study the effect of redshift function $\varphi(r)$ on wormhole solutions within 4 $f(R)$ gravity models. We are seeking solutions that satisfy the WEC, avoid being anti-gravity cases, and steer clear of cosmic instability. To achieve this, in section 2, we began by deriving the field equations in context of $f(R)$ gravity for Morris-Thorne metric. Then, in section 3, we introduced the general forms of our models along with the shape function and the redshift function. We calculated and rewrite the field equations for each model. Continuing into section 3, we found wormhole solutions for each model. In section 4, using the gravitational lensing effect as an observational evident we calculated the effective potential function and by analyzing the deflection angle, we investigated the geodesics around the wormhole.

2 Field equations and wormhole geometry in $f(R)$ gravity

We start with the action of modified $f(R)$ gravity as:

$$S = \frac{1}{2\kappa} \int d^4x \sqrt{-g} (f(R) + \mathcal{L}_M) \quad (2.1)$$

Where \mathcal{L}_M is the Lagrangian of the matter field, $\kappa = 8\pi G$ is the gravitational coupling constant and g is determinant of the metric. In this study, for notational simplicity, we consider $\kappa = 1$. The field equation is derived by varying the action (2.1) with respect to metric $g_{\mu\nu}$, resulting in the following fourth-order field equations [34]:

$$R_{\mu\nu} f_R(R) - \frac{1}{2} g_{\mu\nu} f(R) - (\nabla_\mu \nabla_\nu - g_{\mu\nu} \square) f(R) = \kappa T_{\mu\nu} \quad (2.2)$$

Where $f_R = df(R)/dR$, and $T_{\mu\nu}$ is the energy-momentum tensor that given by varying the matter action S_M with respect to metric $g^{\mu\nu}$:

$$T_{\mu\nu} = \frac{-2}{\sqrt{-g}} \frac{\delta S_M}{\delta g^{\mu\nu}} \quad (2.3)$$

Now, based on the gravitational field equation $G_{\mu\nu} = R_{\mu\nu} - \frac{1}{2}Rg_{\mu\nu}$, we can derive the following equation for Einstein tensor:

$$G_{\mu\nu} = \frac{1}{f_R} \{ f_{RR} \nabla_\mu \nabla_\nu R + f_{RRR} (\nabla_\mu R) (\nabla_\nu R) - \frac{g_{\mu\nu}}{6} (Rf_R + f + 16\pi GT) + 8\pi GT_{\mu\nu} \} \quad (2.4)$$

Here, T represents the trace of the energy-momentum tensor, and f_{RR} and f_{RRR} denote the second and third derivatives of $f(R)$ with respect to R . To have cosmologically viable $f(R)$ gravity models, the following conditions for f_R and f_{RR} need to be satisfied in region $R > R_0$ which R_0 represents the Ricci scalar value at the present background curvature [35]:

a) $f_R > 0$, this is necessary to prevent the occurrence of anti-gravity effects. Note that in this case the wormhole existence condition is violated [33], however these solutions are stable against spherically symmetric perturbations and provides an interesting possibility to construct non-static or thin-shell wormhole solutions [36]

b) $f_{RR} > 0$, to be consistent with local gravity constraints [37] and to maintain the stability of cosmological perturbations [38].

c) $f_{RR} \neq 0$, to prevent the weak singularities which means the divergency in the physical quantities as density and curvature[39]

In the following, we use the Morris-Thorne proposed metric which describes the static and spherically symmetric traversable wormholes [4].

$$ds^2 = -e^{-2\phi(r)} dt^2 + \frac{dr^2}{1 - b(r)/r} + r^2 (d\theta^2 + \sin^2 \theta d\phi^2). \quad (2.5)$$

In this metric, the functions $b(r)$ and $\phi(r)$ are introduced as arbitrary functions of the embedding-space radial coordinate r , which are called the shape function and the redshift function, respectively. The shape function of a wormhole starts from a finite minimum value, which is select as $b(r_0) = r_0$, where r_0 represents the wormhole throat radius. The condition $1 - b(r)/r > 0$ ensures that the signature of the wormhole metric remains consistent. To satisfy the flaring-out condition at or near the throat, we should consider $(b(r_0) - b'(r_0)r_0)/b(r_0)^2 > 0$ [4] or $b'(r_0) < 1$. Since traversable wormholes are examined in this paper which have no horizons therefor the redshift function $\phi(r)$ must be finite everywhere [40]. For the metric (2.5), the Ricci scalar in the case of non-vanishing redshift function is:

$$\begin{aligned} R = & -\frac{2}{r^2} \left[(\varphi(r)'' r^2 + 2\varphi(r)'^2 r^2) \left(1 - \frac{b(r)}{r}\right) - \frac{\varphi(r)'}{2} (b(r)' r - b(r)) - \varphi(r)'^2 r^2 \left(1 - \frac{b(r)}{r}\right) \right. \\ & \left. + 2\varphi(r)' r \left(1 - \frac{b(r)}{r}\right) - r \left(\frac{b(r)'}{r} - \frac{b(r)}{r^2} \right) - \frac{b(r)}{r} \right], \end{aligned} \quad (2.6)$$

We consider anisotropic distribution of matter for which the energy-momentum tensor is in the form[41]:

$$T_{\mu\nu} = (\rho + p_t)U_\mu U_\nu + p_t g_{\mu\nu} + (p_r - p_t) \chi_\mu \chi_\nu, \quad (2.7)$$

where $\rho(r)$ is the energy density and $p_r(r)$ and $p_t(r)$ are the radial and tangential pressures. U^μ is the four-velocity and $\chi^\mu = \sqrt{1 - b(r)/r} \delta_r^\mu$ is the unit spacelike vector in the radial direction. In this paper we investigate the NEC and WEC for the wormhole solutions in the $f(R)$ gravity. These conditions are defined using the formula $T_{\mu\nu}k^\mu k^\nu \geq 0$, where k^μ stands for any null (light-like) vector field for the NEC and any time-like vector field for the WEC [42].

Now, by employing Einstein tensor (2.4), we can calculate $f(R)$ gravity field equations for the wormhole geometry as:

$$\frac{b'(r)}{r^2} f_R = \chi(r) f_{RR} R'(r) \varphi'(r) + \frac{1}{6} (R(r) f_R + f) + \frac{1}{3} (2\rho + 2p_t + p_r), \quad (2.8)$$

$$\begin{aligned} \frac{b(r) + 2r^2 \varphi'(r) \chi(r)}{r^3} f_R &= (R''(r) \chi(r) + \frac{R'(r) \chi'(r)}{2}) f_{RR} + R(r)^{\prime 2} \chi(r) f_{RRR} \\ &+ \frac{1}{6} (R(r) f_R + f) - \frac{1}{3} (\rho + 2p_r - 2p_t), \end{aligned} \quad (2.9)$$

$$\begin{aligned} \left(\varphi''(r) + \varphi'(r)^2 + \frac{\varphi'(r)}{r} - \frac{\chi'(r)(r+1)}{2(r-b)} \right) f_R &= \frac{R'(r)}{r} f_{RR} + \frac{1}{6\chi(r)} (R(r) f_R + f) \\ &- \frac{1}{3\chi(r)} (\rho - p_r + p_t), \end{aligned} \quad (2.10)$$

Here $\chi(r) = \frac{b(r)}{r} - 1$ and prime denotes derivative with respect to r . The field equations (2.8)-(2.10) can be expressed in form of the energy conditions (EC):

$$\begin{aligned} \rho(r) &= \chi(r) R'^2(r) f_{RRR} + \left(\chi(r) R''(r) + \left(\frac{\chi'(r)}{2} + \frac{2\chi(r)}{r} \right) R'(r) \right) f_{RR} \\ &+ \left(\left(\frac{\chi'(r)}{2} + \frac{2\chi(r)}{r} \right) \varphi' - \chi(r) (\varphi''(r) + \varphi'^2(r)) \right) f_R + \frac{f(R)}{2}, \end{aligned} \quad (2.11)$$

$$\begin{aligned} wec_1(r) &= \chi(r) R'^2(r) f_{RRR} + \left((R''(r) - \varphi'(r) R'(r)) \chi(r) + \frac{\chi'(r)}{2} R'(r) \right) f_{RR} \\ &+ \left(\frac{\chi'(r)}{r} - 2 \frac{\varphi'(r)}{r} \chi(r) \right) f_R, \end{aligned} \quad (2.12)$$

$$\begin{aligned}
wec_2(r) &= \chi(r) \left(\frac{1}{r} - \varphi'(r) \right) R'(r) f_{RR} + \left(\left(\frac{\chi'(r)}{2} + \frac{\chi(r) + 1}{r} \right) \left(\frac{1}{r} - \varphi'(r) \right) \right. \\
&\quad \left. - \chi(r) (\varphi''(r) + \varphi'(r)^2) + \frac{\varphi'(r)}{r} \right) f_R,
\end{aligned} \tag{2.13}$$

Where $wec_1(r) = \rho(r) + p_r(r)$, $wec_2(r) = \rho(r) + p_t(r)$. At the wormhole throat we obtain:

$$\rho(r) \Big|_{r=r_0} = \frac{R'(r)}{2r} (b'(r) - 1) f_{RR} - \frac{\varphi'(r)}{2r} (b'(r) - 1) f_R + \frac{f(R)}{2}, \tag{2.14}$$

$$\rho(r) + p_r(r) \Big|_{r=r_0} = \frac{R'(r)}{2r} (b'(r) - 1) f_{RR} + \frac{1}{r^2} (b'(r) - 1) f_R, \tag{2.15}$$

$$\rho(r) + p_t(r) \Big|_{r=r_0} = \left(\frac{1}{2r} (b'(r) + b(r)) \left(\frac{1}{r} - \varphi'(r) \right) + \frac{\varphi'(r)}{r} \right) f_R, \tag{2.16}$$

It is worth to mention that (2.14), (2.15) and (2.16) are in agreement with [19]. Existence of $\varphi(r)$ and its derivatives in Equations (2.14)-(2.16) means that by selecting the adequate redshift function, as we have done in the following, one may find wormhole solutions which respect the NEC and WEC around the wormhole throat.

3 Traversable wormhole solutions in $f(R)$ models

In this section, we are interested in studying WEC and NEC near the throat of wormholes that are the solutions for the equations of the motion of four $f(R)$ gravity models: *I*) Exponential gravity model ([43],[44]) , *II*) Tsujikawa model [45] *III*) Starobisky model [39], *IV*) Hu-Sawicki model [46]. These models, which are consistent with the cosmological observations, can be written in the general form [45]:

$$f(R) = R - \alpha \xi(R) \tag{3.1}$$

In this context, the function $\xi(R)$ are presented in the table 1, designed to satisfy two conditions. First, $\xi(R) \Big|_{R=0} = 0$ our models reduce to the Einstein general relativity. Second, $\xi(R) \Big|_{R \gg R_0} = \text{constant}$ to upholding local gravity constraints where R_0 present background curvature of the universe [47]. The parameter α is a free parameter. In these models, the curvature parameter R_* is a small positive constants [30]. Additionally, λ and n are free positive parameters utilized in these models [45].

Model	$\xi(R)$
Starobisky	$-\lambda R_* [1 - (1 + \frac{R^2}{R_*^2})^{-n}]$
Hu-Sawicki	$-\lambda R_* \frac{(\frac{R}{R_*})^{2n}}{(\frac{R}{R_*})^{2n+1}}$
The exponential gravity	$-\lambda R_* (1 - e^{-\frac{R}{R_*}})$
Tsujikawa	$-\lambda R_* \tanh(\frac{R}{R_*})$

Table 1: $f(R)$ gravity models

In our investigation, we specifically insert the exponential shape function in conjunction with a non-zero redshift function that is characterized by a fractional formula:

$$b(r) = \frac{r}{e^{r-r_0}} \quad (3.2)$$

$$\phi(r) = \frac{\varphi_0}{r^m} \quad (3.3)$$

Where φ_0 is a constant and r_0 is the throat location. The flare-out condition for the shape function (3.2) is checked by the minimality of the wormhole throat as:

$$\frac{d}{dz} \left(\frac{dr}{dz} \right) = \frac{b - b'r}{2b^2} = \frac{1}{2} > 0 \quad (3.4)$$

Inserting the shape function (3.2) and red shift function (3.3), we can rewrite the Ricci scalar (2.6) in the following way:

$$R = -\frac{2m^2\varphi_0^2}{r^{2m+2}}(1 - e^{r_0-r}) + \frac{2m\varphi_0}{r^{m+2}}(1 - m - e^{r_0-r}(1 - m - \frac{r}{2})) + \frac{e^{r_0-r}}{r} \left(\frac{1}{r} - 1 \right) \quad (3.5)$$

Now, by applying the form of $f(R)$ (3.1) in EC equations (2.11)-(2.13), we obtain:

$$\begin{aligned}
wec_1(r) = & \frac{\alpha e^{r_0-r}}{2r^6} \left[\phi_0 m r^{-m} e^{r_0-r} (2r^{-m+1} + r(3m-1) + 4r^{-m}(m+1) + 2(m+2)(m-1) \right. \\
& - 1) - 1 \left. \right]^2 \xi_{RRR} + \frac{\alpha e^{-2(r-r_0)}}{2r^{3m+4}} \left[4r^{3m} \left(e^{r-r_0} (r^3 + r^2 - 2r - 6) - \frac{r^3}{2} - r^2 + r + 6 \right) \right. \\
& + 4\phi_0 m r^{2m} \left(m^3 + (2r+4)m^2 + \left(\frac{5r^2}{4} + 3r + 1 \right) m + \frac{r^3 + 5r^2}{4} - 2r - 8 \right) \\
& - 2 \left(m^3 + (r+4)m^2 + \left(r^2 + \frac{3}{2}r + 1 \right) m + \frac{r^3 + 2r^2}{4} - r - 7 \right) e^{r-r_0} \\
& + e^{2(r-r_0)} (m-1)(m+3)(m+2) + 12\phi_0^2 m^2 r^m \left(m^2 + \left(\frac{r}{2} + 3 \right) m + \frac{7r}{6} + \frac{8}{3} \right. \\
& - 2e^{r-r_0} \left(m^2 + \left(\frac{r}{4} + 3 \right) m + \frac{r^2 + 7r}{12} + \frac{8}{3} \right) + e^{2(r-r_0)} \left(m^2 + 3m + \frac{8}{3} \right) \left. \right) \\
& - 8\phi_0^3 m^3 (e^{r-r_0} - 1) \left((m+1)e^{r-r_0} - m - \frac{r}{2} - 1 \right) \left. \right] \xi_{RR} \\
& - \frac{e^{r_0-r}}{r^{m+2}} \left(r^{m+1} + 2m\phi_0 (e^{r-r_0} - 1) \right) (1 - \alpha \xi_R), \tag{3.6}
\end{aligned}$$

$$\begin{aligned}
wec_2(r) = & \frac{4\alpha(e^{r_0-r} - 1)(\phi_0 m + r^m)}{e^r r^{3m+4}} \left[r^{2m} e^{r_0} \left(\frac{r^2}{2} - 1 \right) + \frac{\phi_0 m r^m}{2} \left((-m^2 - \left(\frac{3r}{2} - 1 \right) m \right. \right. \\
& + (m+2)(m-1)e^r) + \phi_0^2 m^2 \left((m+1)e^r - \left(m + \frac{r}{2} + 1 \right) e^{r_0} \right) \left. \right] \xi_{RR} \\
& - \left[\frac{\phi_0 m}{r^{m+2}} \left((e^{r_0-r} - 1) \left(-\frac{\phi_0 m}{r^m} + m + 1 \right) + 1 \right) \right. \\
& - \left. \frac{r e^{r_0-r}}{1 + \phi_0 m r^{-m}} \left(\frac{-1}{2} + \frac{1}{1 + \phi_0 m r^{-m}} \right) \right] (1 - \alpha \xi_R), \tag{3.7}
\end{aligned}$$

In the limit $\alpha \rightarrow 0$, within the context of Einstein theory, the relation of $wec_1(r)$ (3.6) at the throat $r = r_0$ reveals the violation of the NEC. Consequently, the WEC is also violated at the throat:

$$\rho + p_r \Big|_{r=r_0, \alpha=0} = -\frac{1}{r_0} < 0, \tag{3.8}$$

Due to the advantages of proper length such as its property of invariant measurement, we substitute the shape function (3.2) in the proper length one finds that:

$$l(r) = \pm \int_{r_0}^r \frac{dr}{\sqrt{1 - b(r)/r}} = \pm \ln \left(-\frac{1}{2} + e^{r-r_0} + \sqrt{e^{2(r-r_0)} - e^{r-r_0}} \right) + C, \tag{3.9}$$

Where $C = \pm \ln(2)$. One can also find the reverse function $r(l)$ as:

$$r(l) = \pm \ln \left(\frac{1}{4} + \frac{1}{4} (e^{2l} + 2e^l) \right) + r_0 - l, \tag{3.10}$$

Note that the positive sign corresponds to the upper universe, while the negative sign corresponds to the lower universe and $l = 0$ is equivalent to the throat $r = r_0$. In the following sections, we use the equation (3.10) to plot the energy conditions based on the parameter l .

3.1 Case I: The Exponential gravity model

We begin our investigation with the exponential $f(R)$ gravity model, which represented in the following form [48]:

$$\xi(R) = -\lambda R_*(1 - e^{\frac{R}{R_*}}) \quad (3.11)$$

Where λ is a free positive dimensionless constant and $R_* > 0$ is a curvature parameter [30]. The exponential $f(R)$ model is a valuable tool for describing the dynamics of galactic phenomena [49].

We are interested in wormhole solutions that avoid the anti-gravitating behavior and also without the cosmic instability. To this end we calculate f_R and f_{RR} at the wormhole throat by utilizing the Ricci scalar 3.5:

$$f_R|_{r=r_0} = 1 + \lambda \exp\left(\frac{m\varphi_0}{R_* r_0^{m+1}} - \frac{2}{R_* r_0} \left(\frac{1}{r_0} - 1\right)\right) \quad (3.12)$$

$$f_{RR}|_{r=r_0} = \frac{\lambda}{R_*} \exp\left(\frac{m\varphi_0 r_0^{1-m} - 2r_0 + 2}{R_* r_0^2}\right) \quad (3.13)$$

Equations (3.12) and (3.13) reveal that regardless of the presence or absence of the redshift function, the f_R and f_{RR} are always positive due to the positive values of the free parameters in the model. So in the exponential $f(R)$ model, there is no ghost solutions and we have cosmological stability. In figure (1.a), f_R and f_{RR} are plotted around the throat around the throat when $\varphi_0 = 0$. Note that when $\varphi_0 = 0$, we explore wormhole geometries without the redshift function. In figure (2.a), f_R and f_{RR} are plotted for the case with $\varphi_0 = 1$.

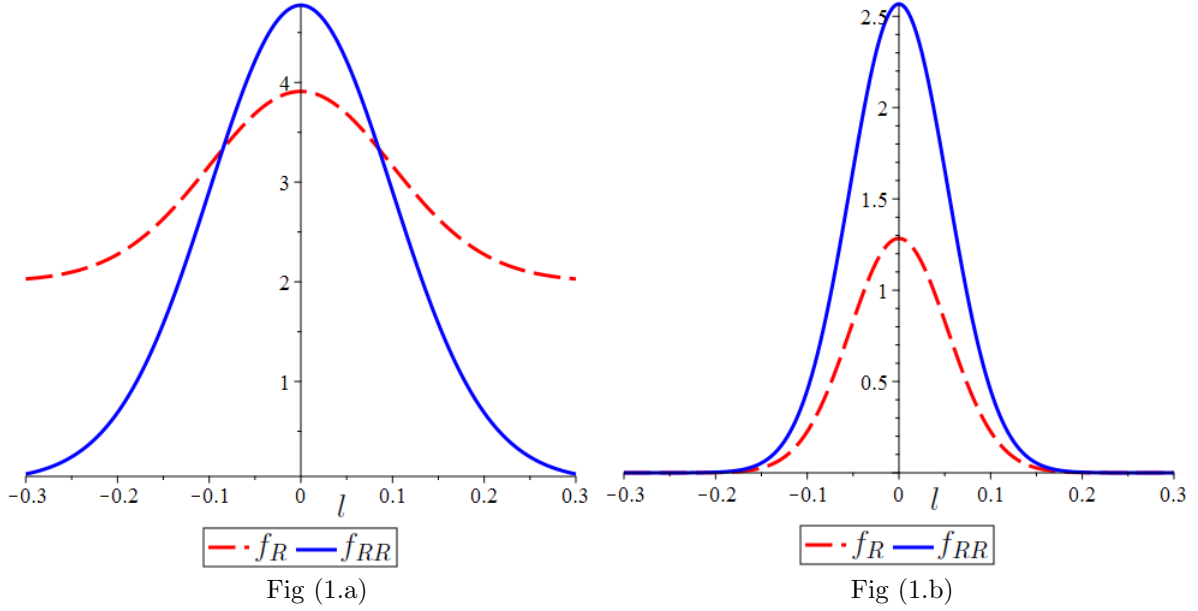


Figure 1: Fig1.a shows that $f_R > 0$ and $f_{RR} > 0$ for the Exponential model with $\varphi(r) = 0$, Fig9.b shows that $f_R > 0$ and $f_{RR} > 0$ when $\varphi_0 = 1$. In these figures we set $\lambda = 0.955$, $R_* = 0.01$, $m = 1$ and $r_0 = 1$.

In the following, we derive the expressions for energy density ρ , wec_1 , and wec_2 at the wormhole throat by using equation (3.6),(3.7):

$$\rho \Big|_{r=r_0} = \frac{1}{2R_*r_0^3} \left[-r_0R_*(R_*\lambda r_0^2 + 2r_0 - 2) + \lambda(\varphi_0 m(1 - R_*)r_0^{2-m} + \varphi_0(3m^2 - m)r_0^{1-m} + 2\varphi_0^2 m^2 r_0^{1-2m} - 2r_0^2 + 4 + R_*^2 r_0^3) e^\eta \right] \quad (3.14)$$

$$wec_1 \Big|_{r=r_0} = \frac{1}{2R_*r_0^3} \left[\lambda(2\varphi_0^2 m^2 r_0^{1-2m} + \varphi_0(3m^2 - m)r_0^{1-m} + \varphi_0 m r_0^{2-m} - 2r_0^2(1 + R_*) + 4) e^\eta - 2r_0^2 R_* \right] \quad (3.15)$$

$$wec_2 \Big|_{r=r_0} = -\frac{\varphi_0 m r_0^{1-m} + r_0 - 2}{2r_0^2} (1 + \lambda e^\eta) \quad (3.16)$$

where $\eta = \frac{\varphi_0 m r_0^{1-m} - 2r_0 + 2}{r_0^2 R_*}$. Using equations (3.14) to (3.16), one can find some conditions to prevent the violation of the NEC and WEC. For instance, equation (3.16) indicates that for $r_0 > 2$ in the absence of the redshift function, the energy conditions will be violated. Ultimately, by choosing appropriate parameters, cases can be found where the energy conditions are maintained. In Figure (2.a), by choosing suitable parameters for a desired case, f_R and f_{RR} are plotted that show no anti-gravity solution. Energy conditions for this case are plotted in figure (2.b) and we can see that NEC and WEC are satisfied.

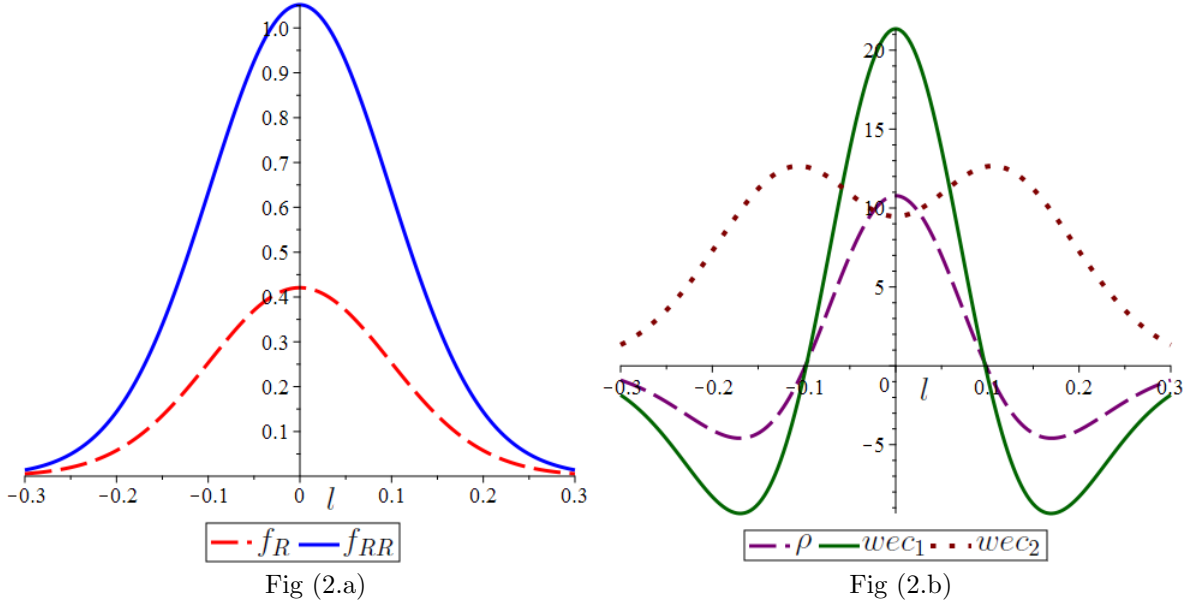


Figure 2: Fig2.a shows that both of f_R and f_{RR} are positive, Fig2.b shows that $\rho(l) > 0$, $wec_1(l) > 0$ and $wec_2(l) > 0$ in the Exponential model. we set $m = 0.1$, $\lambda = 0.955$, $R_* = 0.01$, $r_0 = 1$ and $\varphi_0 = 1$ in these figures.

3.2 Case II: The tsujikawa model

The second $f(R)$ gravity model that we investigate its wormhole solutions is the Tsujikawa model which is given by:

$$\xi(R) = -\mu R_* \tanh\left(\frac{R}{R_*}\right) \quad (3.17)$$

In this model, μ is dimensionless model parameter where $0.905 < \mu < 1$ [45]. The Tsujikawa model can be considered as a similar kind of the exponential $f(R)$ model [50], But due to the difference in its functional structure, it leads to different cosmological results [27].

Similar to previous models, we start by deriving the expressions for the f_R and f_{RR} at the throat to analyze their signs.

$$f_R|_{r=r_0} = \frac{e^{\Omega_1}(e^{\Omega_1} + 2 - 4\mu) + 1}{R_*(e^{\Omega_2} + 1)^2} \quad (3.18)$$

$$f_{RR}|_{r=r_0} = \frac{8\mu e^{\Omega_1}}{R_*(e^{\Omega_2} + 1)^3}(e^{\Omega_1} - 1) \quad (3.19)$$

Where functions Ω_1 and Ω_2 is:

$$\Omega_1 = \frac{2r_0^{-1-m}m\varphi_0r_0^2 - 4(r_0 - 1)}{R_*r_0^2}, \quad \Omega_2 = \frac{2r_0^{1-m}m\varphi_0 - 4(r_0 - 1)}{R_*r_0^2}. \quad (3.20)$$

Based on equations (3.18) and (3.19), the positivity of f_R and f_{RR} depends on the throat radii and constant φ_0 as depicted in figure 3.

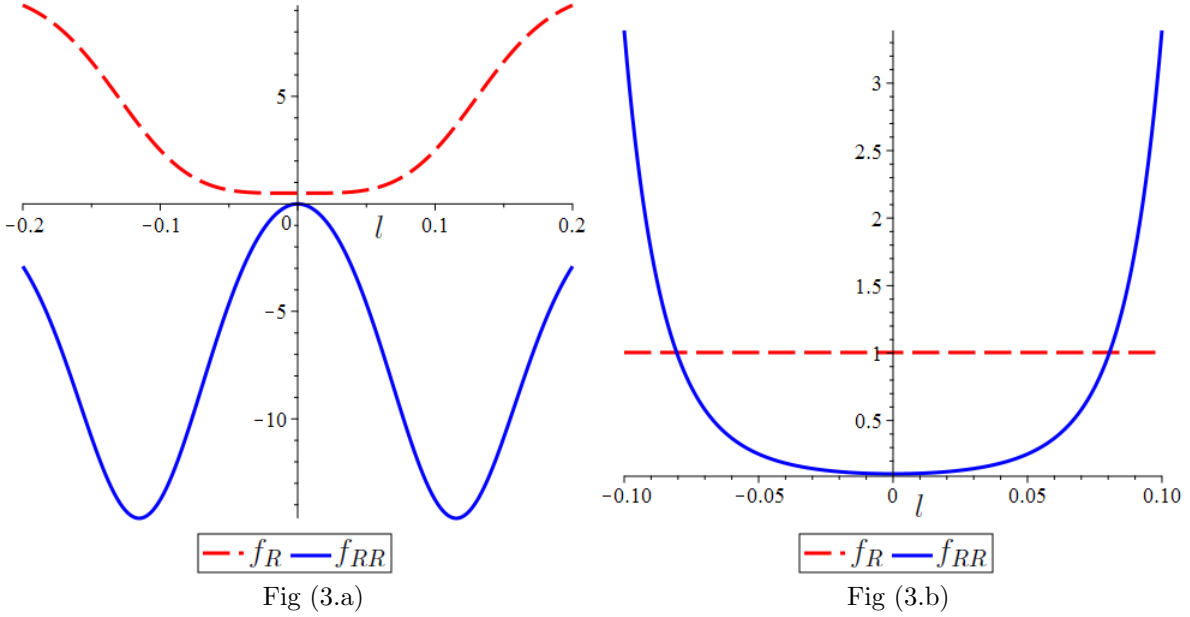


Figure 3: Fig3.a shows that $f_R > 0$, $f_{RR} < 0$ in Tsujikawa model with $\varphi_0 = 0$, Fig3.b shows $f_R > 0$, $f_{RR} > 0$ when $\varphi_0 = 1$, These pictures are plotted by setting $\mu = 0.95$, $R_* = 0.01$ and $r_0 = 1$.

Using equation (3.6), (3.7), we extract the equations for ρ , wec_1 , and wec_2 at the throat of wormhole. We then search for appropriate values that make all these expression positive:

$$\begin{aligned}
\rho|_{r=r_0} &= \frac{1}{2R_*r_0^3\Omega_3^4} [(4m\mu\varphi_0(R_* - 2)r_0^{2-m} - \mu\varphi_0(24m^2 - 8m)r_0^{1-m} - 8r_0R_*(r_0 - 1) \\
&- 16m^2\mu\varphi_0^2r_0^{2m-1} + (2R_*^2r_0^3 + 16r_0^2 - 32)\mu)\Psi(12, 2, 4) + 2(2m\mu\varphi_0(R_* - 2)r_0^{2-m} \\
&- 4r_0R_*(r_0 - 1) + 4\mu\varphi_0(3m^2 - m)r_0^{1-m} + 8m^2\mu\varphi_0^2r_0^{2m-1} - (R_*^2r_0^3 + 8r_0^2 - 16)\mu)\Psi(4, 6, 12) \\
&+ R_*(8mr_0^{2-m}\mu\varphi_0 - 12(r_0 - r_0^2))\Psi(8, 4, 8) + R_*r_0(-R_*\mu r_0^2 - 2r_0 + 2)\Psi(0, 8, 16) \\
&+ R_*r_0(R_*\mu r_0^2 - 2r_0 + 2)\Psi(0, 0, 16)] \quad (3.21)
\end{aligned}$$

$$\begin{aligned}
wec_1|_{r=r_0} &= \frac{1}{R_*r_0^3\Omega_3^4} \left[4\mu(\varphi_0(m - 3m^2)r_0^{1-m} - \frac{r_0^2R_*}{\mu} - 2\varphi_0^2m^2r_0^{1-2m} \right. \\
&- \varphi_0mr_0^{2-m} + (R_* + 2)r_0^2 - 4)\Psi(12, 2, 4) + 4\varphi_0\mu((3m^2 - m)r_0^{1-m} \\
&+ 2\varphi_0^2m^2r_0^{1-2m} + mr_0^{2-m} + (R_* - 2)r_0^2 + 4 - \frac{r_0^2R_*}{\mu})\Psi(4, 6, 12) \\
&\left. - R_*r_0^2((6 - 8\mu)\Psi(8, 4, 8) + \Psi(0, 0, 16) + \Psi(0, 8, 16)) \right] \quad (3.22)
\end{aligned}$$

$$\begin{aligned}
wec_2|_{r=r_0} &= \frac{2 - \varphi_0mr_0^{1-m} - r_0}{2r_0^2\Omega_3^3} \left[e^{4r_0+8}(3 - 4\mu)(\Psi(0, 4, 0) + \Psi(4, 2, -4)) \right. \\
&\left. + \Psi(0, 0, 12) + \Psi(0, 6, 12) \right] \quad (3.23)
\end{aligned}$$

where the function Ω_3 and $\Psi(a_1, a_2, a_3)$ defined as:

$$\Omega_3 = \exp\left(\frac{2\varphi_0 m r_0^{1-m} + 4}{r_0^2 R_*}\right) + \exp\left(\frac{4}{r_0 R_*}\right) \quad (3.24)$$

$$\Psi(a_1, a_2, a_3) = \frac{\exp(a_1 r_0 + a_2 \varphi_0 m r_0^{-1-m} r_0^2 + a_3)}{\exp(r_0^2 R_*)} \quad (3.25)$$

It is evident from the figure 4 that by selecting a suitable φ_0 , NEC and WEC are respected alongside the conditions for cosmological stability and the absence of ghost solutions.

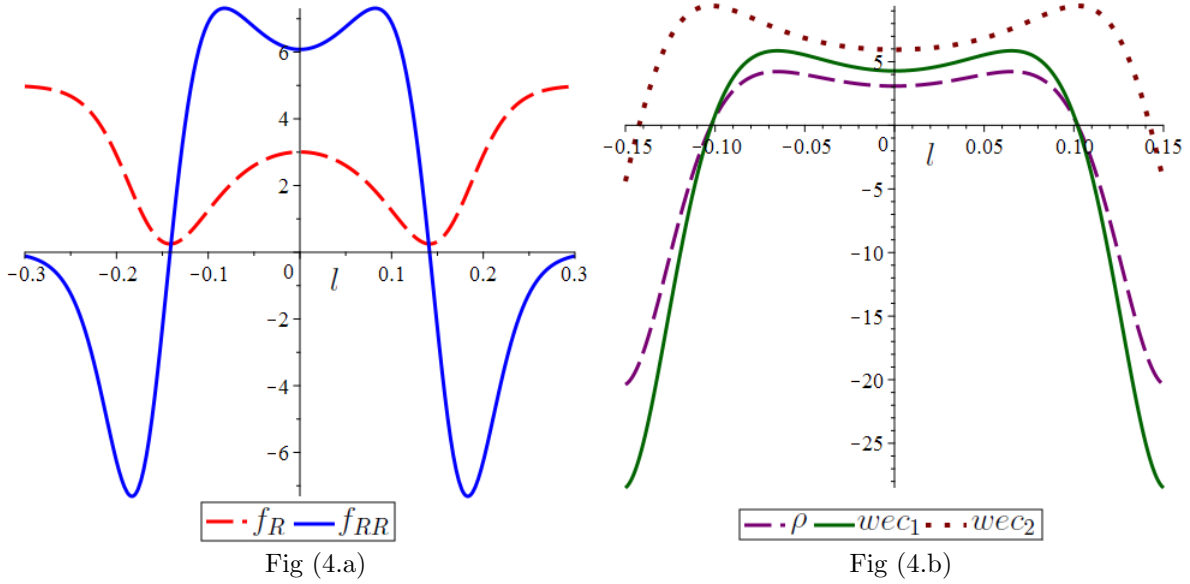


Figure 4: Fig4.a shows that $f_R > 0$, $f_{RR} > 0$ in Tsujikawa model in the presence of redshift function, Fig4.b shows $\rho(l) > 0$, $wec_1(l) > 0$ and $wec_2(l)$, These pictures are plotted by setting $\varphi_0 = 0.01$, $\mu = 0.95$, $R_* = 0.01$ and $r_0 = 1$.

3.3 Case III: The Starobinsky gravity model

Another model that we consider here is the Starobinsky model [39]. This is a viable modified $f(R)$ gravity model with three free parameters R_S , λ and n [45]:

$$\xi(R) = -\lambda R_* \left[1 - \left(1 + \frac{R^2}{R_s^2}\right)^{-n}\right] \quad (3.26)$$

Where λ is a positive dimensionless parameter which is in the range $0.944 < \lambda < 0.966$ for $n = 2$ [45] and R_* is a curvature parameter which takes small positive value [30]. The Starobinsky model is one of the important models which describe the cosmic inflation and is consistent with the observations such as the solar system dynamics. Like the two previous models, we are searching for solutions that satisfy NEC and WEC. However, due to the messy

form of equations of energy conditions, in this section, we have presented all equations for a specific value of m equal to one. By taking λ in the mentioned interval, it is possible to find wormholes that respect NEC and WEC. Considering the vanishing redshift function, one finds that at the wormhole throat ($l = 0$), f_R is positive and f_{RR} is negative which shows that without Redshift function the Starobisky model is unstable despite the absence of ghost solutions:

$$f_R|_{r=r_0} = 1 + 4n\lambda R_*^{1-2n} r_0^{2-4n} \sigma_1 (R_*^2 r_0^4 + 4\sigma_1^2)^{-n-1} \quad (3.27)$$

$$f_{RR}|_{r=r_0} = \frac{1}{R_*^2 r_0^4 + 4\sigma_1^2} \left[2nr_0^4 \lambda (-R_*^2 r_0^4 + 2(2n+1)\sigma_1^2) + R_* \left(1 + \frac{4\sigma_1^2}{R_*^2 r_0^4}\right)^{-n} \right] \quad (3.28)$$

where $\sigma_1 = r_0 - 1 - \frac{\varphi_0}{2}$. In figures (5.a) and (5.b), the f_R and f_{RR} are plotted in terms of l , in the vicinity of wormhole throat. In both cases, the f_R is positive, so that we do not have anti-gravity solutions for traversable wormholes. Note that f_{RR} is negative around the throat in figure (5.a), while by applying the redshift function it becomes positive, resulting in stable cosmological perturbations for our Morris-Thorne wormhole solution as shown in figure (5.b).

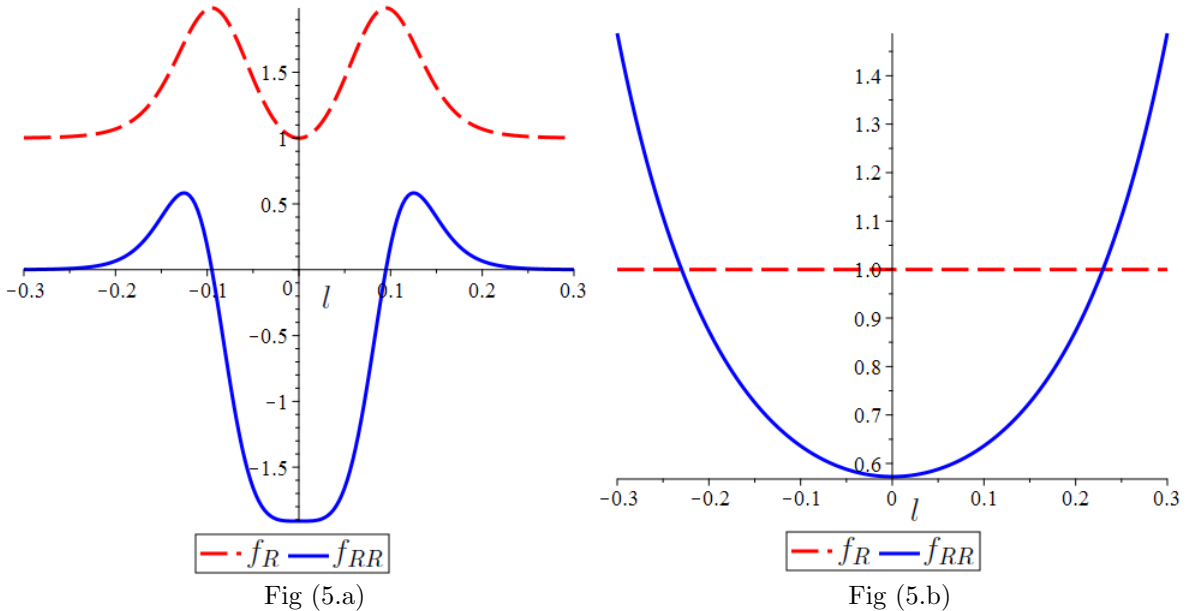


Figure 5: Fig5.a shows that $f_R > 0$, $f_{RR} < 0$ for Starobisky model when $\phi(r) = 0$, Fig5.b shows that both of f_R and f_{RR} are positive with non-vanishing redshift. we set $R_* = 0.01$, $n = 2$, $\lambda = 0.955$, $\varphi_0 = 1$ and $m = 1$.

By applying equations (3.6) and (3.7), the energy conditions for the wormhole solutions of this model are:

$$\begin{aligned}
\rho|_{r=r_0} &= \frac{\sigma_2}{\sigma_3} \left[32\lambda R_* r_0^2 \sigma_1^2 (r_0^3 - \varphi_0^2 - (\frac{r_0^2}{2} + r_0)\varphi_0 - 2r_0)n^2 + 4\lambda R_* (\frac{3\varphi_0^4}{2} + \varphi_0^3(\frac{r_0^2}{2} - 6r_0 + 7)) \right. \\
&+ (8r_0^2 - \frac{r_0^4 R_*^2}{2} - 3r_0^3 - 14r_0 + 10)\varphi_0^2 + r_0^2 n(4 - \frac{R_*^2 r_0^6}{2} - 2r_0^5 R_*^2 + (R_*^2 + 6)r_0^4 - 8r_0^3 - 2r_0^2)\varphi_0 \\
&\left. + (r_0^3 - 2r_0)(R_* r_0^2 + 2r_0 - 2)(R_* r_0^2 - 2r_0 + 2) + \frac{\sigma_3}{2\sigma_2 r_0^2} (2(1 - r_0) + \lambda R_* r_0^2 (\sigma_2 - 1)) \right], \quad (3.29)
\end{aligned}$$

$$\begin{aligned}
wec_1|_{r=r_0} &= \frac{1}{2\sigma_3(1 - r_0^2)} \left[\frac{\sigma_3}{2r_0^2} - n\lambda R_* r_0 \sigma_3 ((-2R_*^2 r_0^7 - R_*^2 r_0^6 (\varphi_0 + 4) + (16n + 8)r_0^5) \right. \\
&+ (2R_*^2 \varphi_0^2 - (24n + 12)\varphi_0 - 32n)r_0^4 + 12r_0^3 (\varphi_0 + 2) (\frac{2n + 1}{2}\varphi_0 - \frac{2n + 7}{3}) + (8(1 - n)\varphi_0^2 \\
&- (2n + 1)\varphi_0^3 + (56n + 76)\varphi_0 + 32n + 80)r_0^2 + 4r_0(\varphi_0 + 2)((3n + 1)\varphi_0^2 - 4(n + 1)(\varphi_0 + 1)) \\
&\left. - 2((2n + 1)\varphi_0^2(\varphi_0 + 2)^2) \right], \quad (3.30)
\end{aligned}$$

$$wec_2|_{r=r_0} = \frac{r_0 + \varphi_0 - 2}{\sigma_3} (2\sigma_1^2 + 2\lambda R_* r_0^2 n \sigma_1 \sigma_2 + R_*^2 r_0^4), \quad (3.31)$$

where σ_2 and σ_3 defined as:

$$\sigma_2 = \left(1 + \left(\frac{2r_0 - \varphi_0 - 2}{R_* r_0^2}\right)^2\right)^{-n}, \quad \sigma_3 = 2r_0^2 (r_0^4 R_*^2 + (\varphi_0 - r_0 + 1)^2 + 3(r_0 - 1)^2)^2. \quad (3.32)$$

As evident from equations (3.29-3.31), in each desired throat radius, with the appropriate determination of the value of φ_0 , related to the redshift function, a stable cosmological wormhole solution can be found that satisfies all three equations and avoids non-gravitational solutions (figure6).

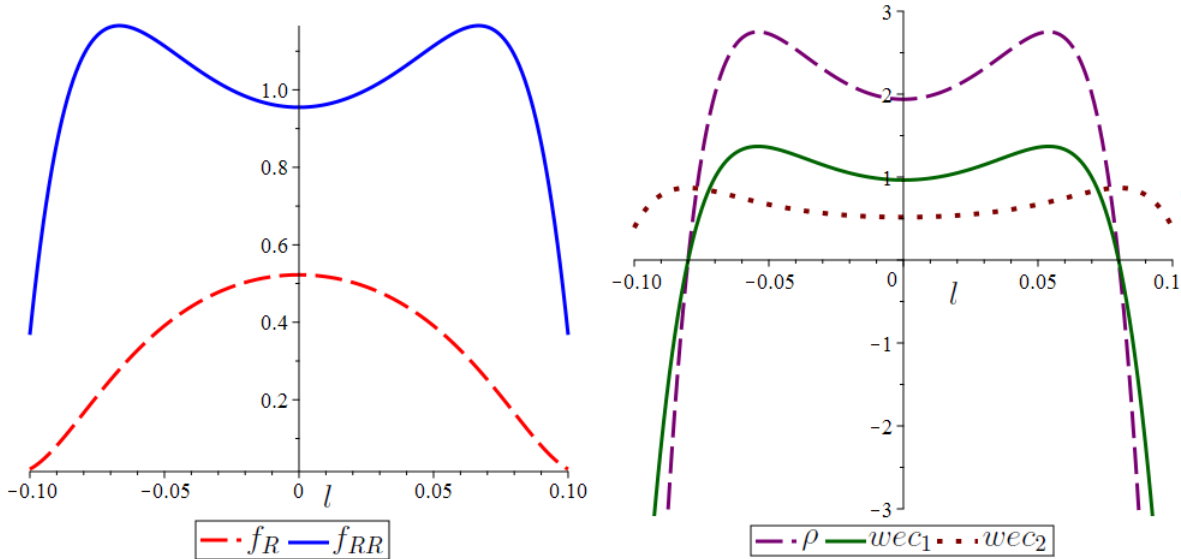


Fig (6.a)

Fig (6.b)

Figure 6: Fig6.a shows that $f_R > 0$, $f_{RR} > 0$. Fig6.b shows that $\rho(l) > 0$, $wec1(l) > 0$ and $wec2(l) > 0$. we set $m = 1$, $\varphi_0 = 0.01$, $n = 2$, $\lambda = 0.955$, $R_* = 0.01$ and $r_0 = 1$

We also explored the outcomes for various values of m . Our findings indicate that in the Starobinsky model, the general behavior of f_R , f_{RR} and the energy conditions remain consistent regardless of the parameter m .

3.4 Case IV: The Hu-Sawicki model

The last modified gravity model that we consider here, is a cosmologically viable model proposed by Hu and Sawicki [46] which is in the form:

$$\xi(R) = -\lambda R_* \frac{\left(\frac{R}{R_*}\right)^{2n}}{\left(\frac{R}{R_*}\right)^{2n} + 1} \quad (3.33)$$

Where n , λ and R_* are positive parameters. The Hu-Sawicki model satisfies cosmological and local gravity constraints. In [45], The range of parameters are investigated. It is shown that for $n = 1$ one should insert $\lambda \geq 8\sqrt{3}/9$. Similar to the previous models, in the first step, we compute f_R and f_{RR} at the wormhole throat but due to the messy form of the energy conditions equation, in the following, we have presented all calculations in the specific case where $m = 1$:

$$f_R|_{r=r_0} = \frac{(R_* \lambda n r_0^2 + 2\gamma_1^2)\gamma_2^{2n} + \gamma_1^2(\gamma_2^{4n} + 1)}{\gamma_1^2(\gamma_2^{2n} + 1)^2} \quad (3.34)$$

$$f_{RR}|_{r=r_0} = \frac{-2R_* \lambda n r_0^4}{4\gamma_1^2(\gamma_2^{2n} + 1)^3} (2n(\gamma_2^{2n} - \gamma_2^{4n}) - \gamma_2^{2n} - \gamma_2^{4n}) \quad (3.35)$$

where $\zeta(r_0)$ and $D(r_0)$ defined as:

$$\gamma_1 = r_0 - 1 - \frac{\varphi_0}{2}, \quad \gamma_2 = \frac{-2\zeta(r_0)}{r_0^2 R_*}. \quad (3.36)$$

Considering (3.34) and (3.35), one can determine the sign of f_R and f_{RR} for different values of the r_0 . Our research indicates that within suitable radii of the throat which satisfied energy conditions, when the redshift function is absent, the f_{RR} is negative which resulted to cosmic instability. However, by inserting the redshift function, we can find cases where both of f_R and f_{RR} turn positive (Figure 7).

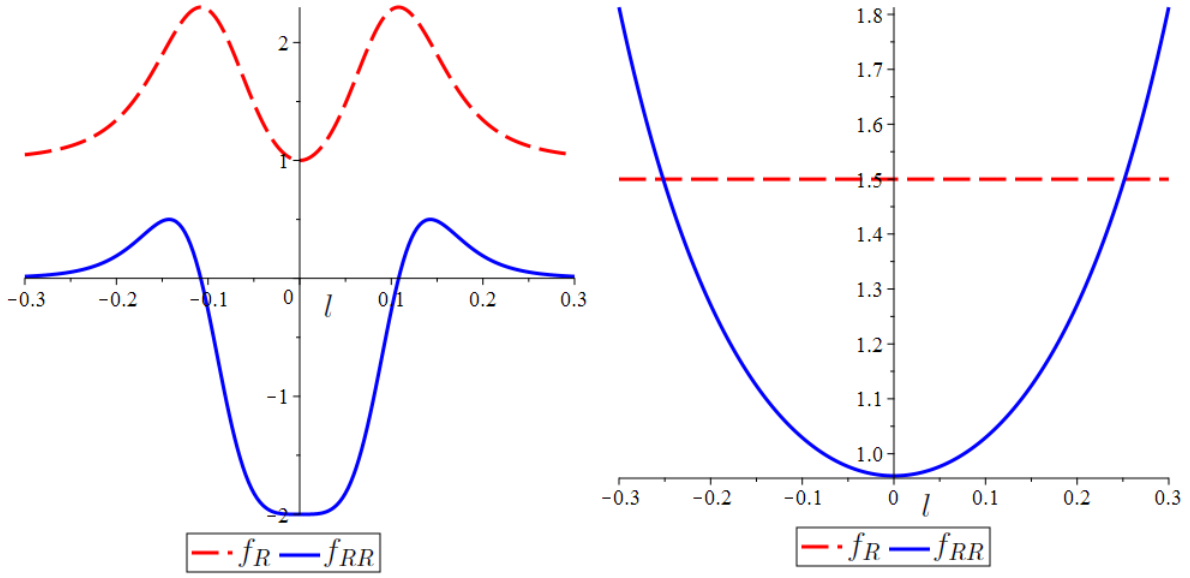


Fig (7.a)

Fig (7.b)

Figure 7: Fig7.a shows that $f_R > 0, f_{RR} < 0$ for Hu-Sawicki model when $\phi(r) = 0$. Fig7.b shows that $f_R > 0, f_{RR} > 0$ when utilizing $\varphi(r) = \frac{1}{r}$. In these cases we set $n = 1, \lambda = 2, R_* = 0.01$ and $r_0 = 1$.

Using (3.6) and (3.7), it is straightforward to rewrite ρ, wec_1 and wec_2 in the following form which, due to their complexity, have been set $m = 1$:

$$\begin{aligned} \rho|_{r=r_0} &= \frac{1}{2r_0^2\gamma_1^2(\gamma_2^{2n} + 1)^4} [(nr_0^2\lambda R_*(2n\gamma_3 - \gamma_4) - (R_*\lambda r_0^2 + 8r_0 - 8)\gamma_1^2)\gamma_2^{2n} \\ &- (2r_0^2\gamma_4\lambda R_*n + 3\gamma_1^2(R_*\lambda r_0^2 + 4r_0 - 4))\gamma_2^{4n} - (2r_0^2\gamma_3\lambda R_*n^2 - r_0^2\gamma_4\lambda R_*n \\ &+ 3\gamma_1^2(r_0^2R_*\lambda + \frac{3}{2}(r_0 - 1)))\gamma_2^{6n} - 4(r_0^2\gamma_2^{8n}R_*\lambda + 2(r_0 - 1)(\gamma_2^{8n} + 1))\gamma_1^2] \end{aligned} \quad (3.37)$$

$$\begin{aligned} wec_1|_{r=r_0} &= \frac{1}{r_0\gamma_1^2(\gamma_2^{2n} + 1)^4} [(\frac{n}{2}\lambda r_0 R_*(\gamma_3(n - 1) - 2r_0(r_0 - 1)) \\ &- 4\gamma_1^2)(\gamma_2^{2n} - \gamma_2^{6n}) - (\lambda r_0(\gamma_3 + 2r_0^2 - 2r_0)R_*n - 6\gamma_1^2)\gamma_2^{4n} - 2\gamma_1^2(\gamma_2^{8n} + 1)] \end{aligned} \quad (3.38)$$

$$wec_2|_{r=r_0} = \frac{2 - r_0 - \varphi_0}{2r_0^2\gamma_1^2(\gamma_2^{2n} + 1)^3} [(\lambda r_0^2 R_* n + 3\gamma_1)(\gamma_2^{2n} + \gamma_2^{4n}) + \gamma_1^2(\gamma_2^{6n} + 1)] \quad (3.39)$$

where $\gamma_3 = -\varphi_0^2 - (\frac{1}{2}r_0^2 + r_0)\varphi_0 + r_0^3 - 2r_0$ and $\gamma_4 = (r_0^3 - \frac{1}{2}\varphi_0 r_0^2 - \frac{3}{2}\varphi_0^2 - 2r_0 - \varphi_0)$. By setting suitable parameters and considering appropriate φ_0 in each throat radius r_0 , one can find geometries where the NEC and WEC are satisfied.

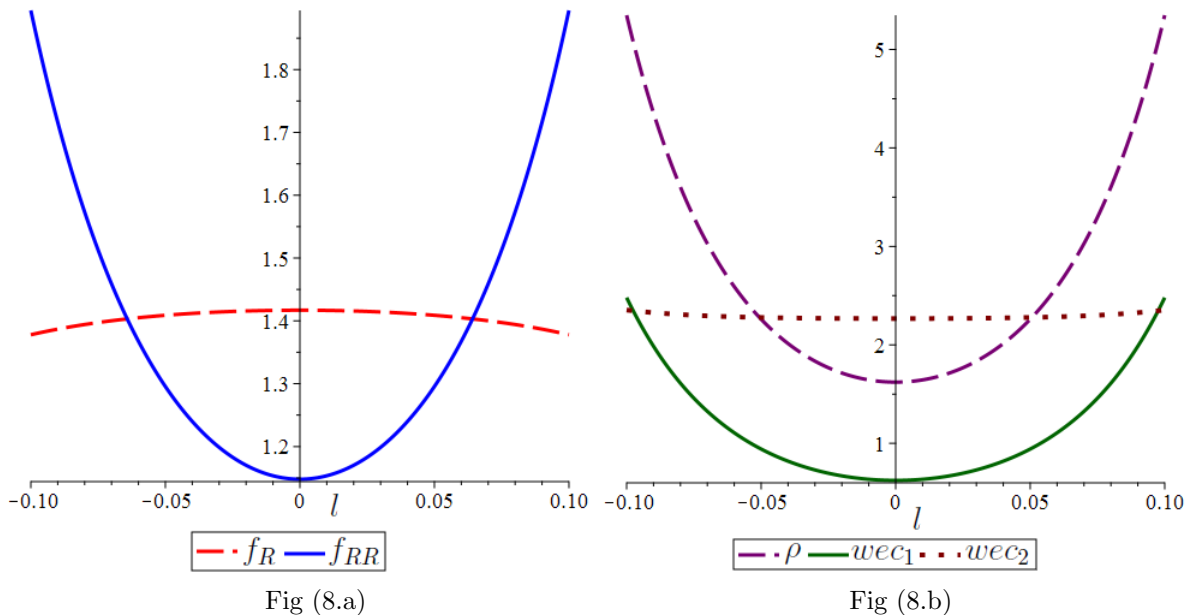


Figure 8: Fig8.a shows that $f_R < 0$ and $f_{RR} > 0$ results in anty-gravity solutions Fig8.b shows that $\rho(l) > 0, wec_1(l) > 0$ and $wec_2(l) > 0$ at the throat and its vicinity. In these figures, we set $\varphi_0 = 0.04$, $n = 1$, $\lambda = 2$, $R_* = 0.01$ and $r_0 = 1$.

We also examined the results for different values of m . We found that in the Hu-Sawicki model, the generic behavior of f_R , f_{RR} and energy conditions are independent of the parameter m .

4 Gravitational lensing and Particle Trajectories Around the Wormhole

The curved space-time around a wormhole can deflect the light rays and affects the particle trajectories. In this section, by using the effective potential, we find the path of particles around the wormholes. We also analyze the gravitational lensing in the case of f(R) wormholes.

4.1 Effective Potential

First, using the Lagrangian formalism, we calculate the effective potential by using the particle trajectories around the wormhole. Taking spherical symmetry and considering the equatorial plane $\theta = \frac{\pi}{2}$, Lagrangian for the metric (2.5) is written as: [51]:

$$\mathfrak{L} = g_{\mu\nu}\dot{x}^\mu\dot{x}^\nu = -e^{2\phi(r)}\dot{t}^2 + \frac{\dot{r}^2}{1 - \frac{b(r)}{r}} + r^2\dot{\phi}^2 \quad (4.1)$$

Where dot refers to the first-order derivative with respect to the affine parameter η . The Lagrangian (4.1) on a geodesic is constant which we demonstrate it by $\mathfrak{L}(x^\mu, \dot{x}^\mu) = \epsilon$. When $\epsilon = -1$ and $\epsilon = 0$ a time-like and null geodesics exists, respectively. Using the Euler-Lagrange equation:

$$\frac{d}{d\eta} \frac{\partial \mathfrak{L}}{\partial \dot{x}^\mu} - \frac{\partial \mathfrak{L}}{\partial x^\mu} = 0, \quad (4.2)$$

For a test particle with energy E and angular momentum L one can derive the following constants of motion:

$$-e^{2\phi(r)}\dot{t} = E, \quad 2r^2\dot{\phi} = L. \quad (4.3)$$

By replacing the motion constants (E and L) into the equation (4.1), we obtain:

$$\dot{r}^2 = e^{-2\phi(r)}\left(1 - \frac{b(r)}{r}\right)\left(E^2 - \frac{L^2}{r^2}\right). \quad (4.4)$$

Using the proper radial distance(3.9), constants of motion(4.3) can be written as:

$$\dot{l}^2 + V_{eff}(L, l) = E^2, \quad (4.5)$$

Where V_{eff} is the effective potential which determined:

$$V_{eff}(L, l) = e^{2\phi(l)}\left(\frac{l^2}{r(l)^2} - \epsilon\right), \quad (4.6)$$

By comparing the effective Potential and total energy E of the particle, the possibility of the particle passing through the wormhole throat can be investigated. If $E^2 > V_{eff}(L, 0)$, the particle passes through the throat and enters another world, otherwise it returns to the primary world when $E^2 < V_{eff}(L, 0)$. In such scenarios, a significant point to consider is the existence of a turning point, denoted as $l = l_o$, which can be determined by solving the following equation:

$$E^2 = V_{eff}(L, l_o). \quad (4.7)$$

$V_{eff}(L, l)$ is plotted against l for null (figure 9.a) and timelike (figure 9.b) geodesics. We investigated the results for different L when $\varphi_0 > 0$. As illustrated in figure 9, Increasing the value of L results in escalation of $V_{eff}(L, 0)$.

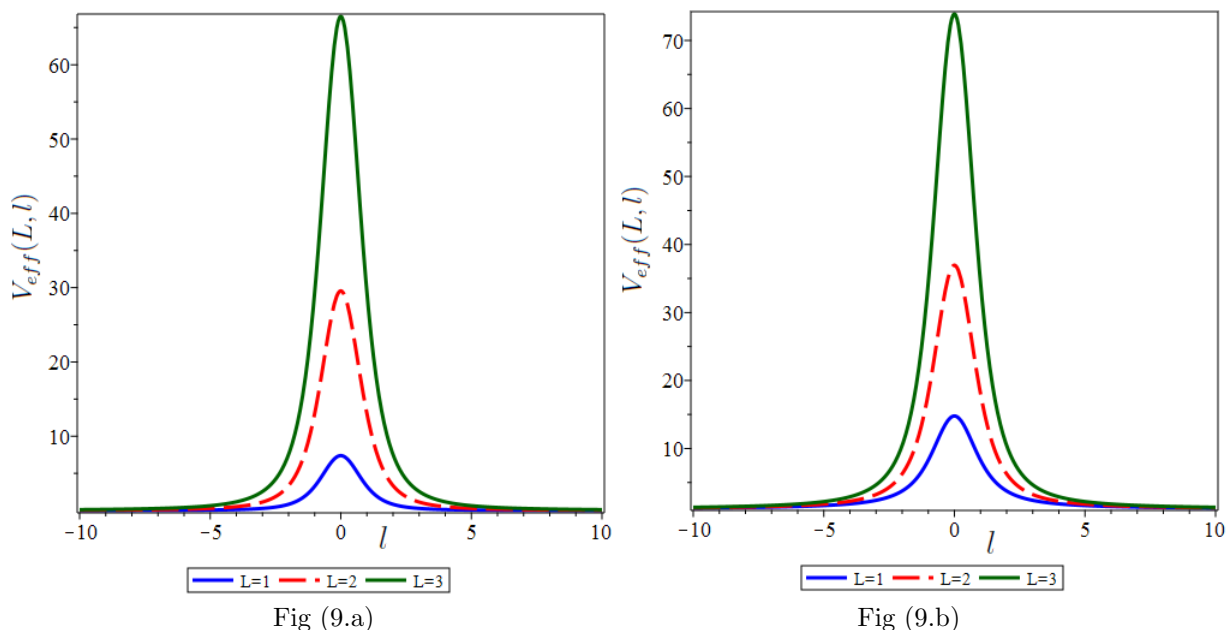


Figure 9: Fig9.a shows $V_{eff}(L, l)$ in null geodesics, Fig9.b shows $V_{eff}(L, l)$ for timelike geodesics. these curves plot by setting $\varphi_0 = 1$, $r_0 = 1$ and L has three values= 1, 2, 3.

As we can see from Figure 9, the pattern of effective potential is the same for both timelike or null geodesics, note that the maximum of $V_{eff}(L, l)$ increases with the growth of L . This means that if the $E^2 = V_{eff}(L, 0)$ then the particle will move in an unstable circular orbit at the location of wormhole throat.

$V_{eff}(L, l)$ is plotted against l when $\varphi_0 < 0$ for null (figure 10.a) and timelike (figure 10.b) geodesics. By comparing figures 13.a and 13.b, it is evident that the $V_{eff}(L, l)$ in null geodesics shows different behavior from timelike geodesics. In null geodesics with increasing L the shape of does not change, but in timelike geodesics with increasing L the $V_{eff}(L, l)$ reaches a relative minimum that creates a state which cause particles to be trapped in the throat of wormhole and revolve on a stable circular orbit.

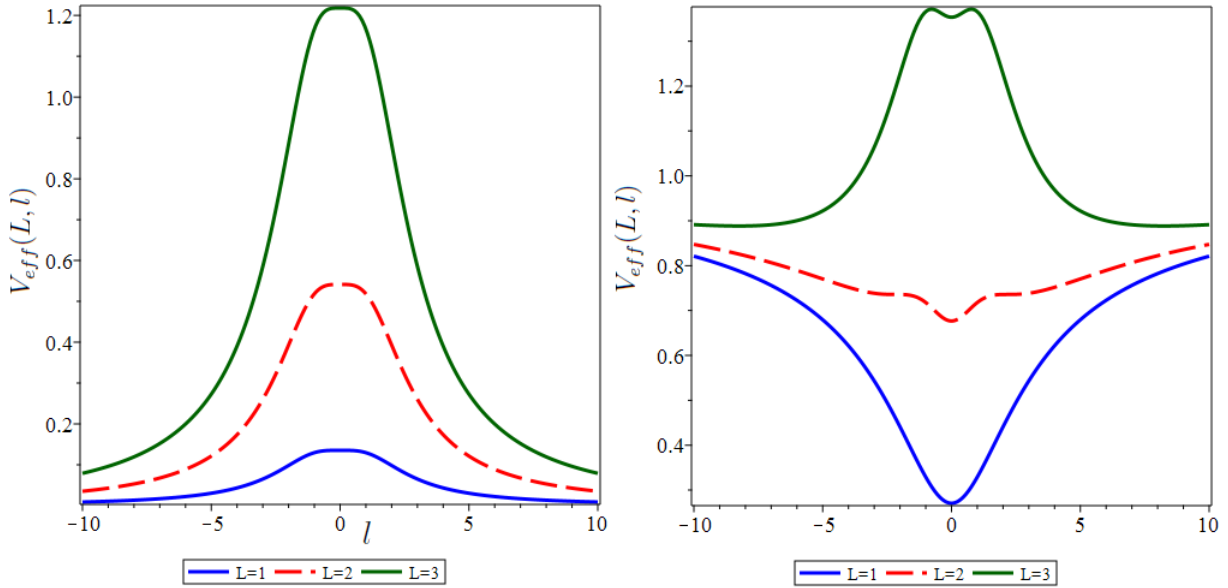


Fig (10.a)

Fig (10.b)

Figure 10: Fig10.a shows $V_{eff}(L, l)$ in null geodesics, Fig10.b shows $V_{eff}(L, l)$ for timelike geodesics. these curves plot by setting $\varphi_0 = -1$, $r_0 = 1$ and L has three values:1, 2, 3.

4.2 The Deflection Angle

When a beam of light passes from infinity to near a massive object like a blackhole, it bends from its direct route and approaches the center of gravitational body to distance r_c . A wormhole has a strong gravitational field, so it acts like a gravitational lens and diverts beam of light. The closest path of light near the throat is r_c . As gravitational field be stronger, the deflection of light beam be greater. The Deflection Angle $\Theta(r_c)$ is a good observational measurement of light bending and obtain from following relation for a Morris-Thorne Wormhole metric (2.5) [52]:

$$\Theta_{r_c} = -\pi + 2 \int_{r_c}^{\infty} \frac{e^{\phi(r)} dr}{r^2 \sqrt{\left(1 - \frac{b(r)}{r}\right) \left(\frac{1}{\beta^2} - \frac{e^{2\phi(r)}}{r^2}\right)}}, \quad (4.8)$$

Where β is Imapct factor and and we have $\beta = r_c e^{-\phi(r_c)}$ for null geodesics. By replacing β , the shape function (3.2) and the redshift function (3.3) in deflection angle (4.8), we obtain:

$$\Theta_{r_c}(\phi_0, m) = -\pi + 2 \int_{r_c}^{\infty} \frac{e^{\phi_0/r^m} dr}{r^2 \sqrt{\left(1 - \frac{1}{e^{r-r_0}}\right) \left(\frac{e^{2\phi_0/r_c^m}}{r_c^2} - \frac{e^{2\phi_0/r^m}}{r^2}\right)}}, \quad (4.9)$$

In the following, we plot the deflection angle Θ_{r_c} according to r_c for three different values of m . Figure 11 shows that in $r_0 < r_c < \infty$, the deflection angle has finite quantity,

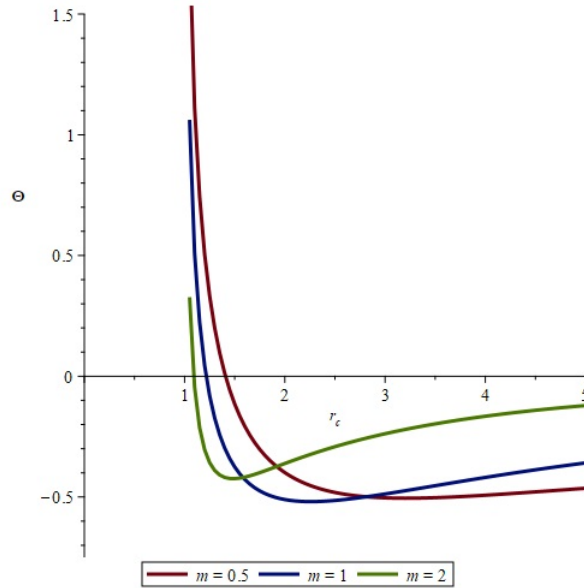


Figure 11: shows the deflection angle for 3 values of parameter m , we set $\varphi_0 = 1$ and $r_0 = 1$.

and as the distance r_c decreases to the wormhole throat, the deflection angle increases. In other words, as the light ray closes to the wormhole throat, where the gravitational field is stronger, its deflection from the original path will be more pronounced. In the wormhole throat, where the gravitational field is extremely strong, the deflection angle tends to infinity. When r_c increases to infinity, the deflection angle tends to zero. Figure 11 also illustrates when $r_c \rightarrow \infty$, for larger values of m the angle of deflection approaches to zero sooner. as shown in figure 11, the value of the parameter m increases, the deflection angle of the light ray near the throat decreases. Conversely, for smaller values of m , the deflection angle near the wormhole throat becomes larger.

5 Conclusions

In this article, we investigate wormhole solutions with non-vanishing redshift function in the framework of $f(R)$ gravity. First, we solved the field equations and then by inserting the exponential shape function and a fractional redshift function we analyzed the wormhole solutions by considering different cosmological viable $f(R)$ models. We rewrote the radial coordinate r in terms of the proper length l and investigated NEC and WEC at the vicinity of wormhole throat. we also took into account the positivity of f_R and f_{RR} to avoid gravitational ghosts and cosmological instability in the solutions. By choosing suitable parameters of each model and redshift function, we looked for the wormhole solutions without the need to exotic matter. We also examined the effective gravitational potential for null and time-like

geodesics. Finally, we calculated the deflection angle near the wormhole structures to analyze gravitational lensing. In the following we review the results for these $f(R)$ models:

case *I*: The Exponential model

Considering the applied redshift function, both the f_R and f_{RR} will always be positive. Therefore, the exponential gravity model, does not contain ghost solutions and also our solutions remain cosmologically stable. By selecting appropriate parameters φ_0 and m , we found the wormhole solutions that satisfy NEC and WEC, here the parameters λ and R_* have no considerable influence on the behavior of energy conditions.

case *II*: The Tsujikawa model

In the Tsujikawa model, contrary to the previous model, the f_R and f_{RR} are not always positive. Particularly, f_{RR} is negative in many cases. However, by inserting the redshift function with suitable values of φ_0 and m , it is possible to find wormhole geometries with cosmological stability. The only free parameter in the Tsujikawa model, μ , has no effect on the satisfaction of the energy conditions and it is easy to find solutions that satisfy NEC and WEC alongside the positivity of f_R and f_{RR} by introducing the redshift function and setting the adequate parameters for it.

case *III*: The Starobinsky model

The positivity of f_R and f_{RR} and the satisfaction of NEC and WEC in the Starobinsky model depend on the selection of appropriate parameters and inserting the redshift function facilitates this process. The free parameters of the model n and λ , do not significantly influence the attainment of the desired solutions. In fact we found the the best way to construct wormhole solutions which respect the NEC and WEC is choosing adequate values for φ_0 .

case *IV*: The Hu-Sawicki model

The behavior of the Hu-Sawicki model resembles that of the Starobinsky model. By selecting appropriate φ_0 in the redshift function, we were able to find wormhole geometries where the NEC and WEC are satisfied, and the f_R and f_{RR} become positive.

As a final remark, our results showed that incorporating the redshift function into wormhole solutions has a substantial impact on their behavior. Certainly, Introducing the redshift function $\varphi(r)$ prevents the f_{RR} from becoming negative in the tsujikawa, Strabinsky and Hu-sawicky models. Furthermore, by examining the value of the parameters φ_0 in the $\varphi(r)$, we can find wormhole solutions that exist without the need for exotic matter. These solutions are stable against spherically symmetric perturbations and provides an interesting possibility to construct non-static or thin-shell wormhole solutions[53] in the considered $f(R)$ gravity models.

Acknowledgment

References

- [1] L. Flamm, Phys. Z. 17, 448 (1916).
- [2] A. Einstein and N. Rosen, Phys. Rev. 48, 73 (1935).
- [3] C. W. Misner and J. A. Wheeler, Ann. Phys. **2**, 525 (1957);
C. W. Misner, Phys. Rev. **118**, 1110 (1959).
- [4] M. S. Morris and K. S. Thorne, Am. J. Phys. 56, 395 (1988).
M. S. Morris, K. S. Thorne and U. Yurtsever, Phys. Rev. Lett. 61, 1446 (1988).
- [5] S. Kar, N. Dadhich, and M. Visser, Pramana J. Phys. 63, 859 (2004);
D. Hochberg and M. Visser, Phys. Rev. D 56, 4745 (1997).
- [6] S. M. Carroll, Living Rev. Rel. 4, 1 (2001);
P. J. E. Peebles and B. Ratra, Rev. Mod. Phys. 75, 559 (2002);
V. Sahni, Class. Quantum Grav. 19, 3435 (2002);
T. Padmanabhan, Phys. Rep. 380, 235 (2003);
P. F. Gonzales-Diaz, Phys. Rev. D 65, 104035 (2002).
- [7] M. Visser, Nucl. Phys. B328, 203-212 (1989);
M. Visser, Phys. Rev. D39, 3182-3184 (1989);
N. M. Garcia, F. S. N. Lobo and M. Visser, Phys. Rev. D86, 044026 (2012).
- [8] T. Clifton, P. G. Ferreira , A. Padilla and C. Skordis, Modified gravity and cosmology,
Physics Reports 513 1189 (2012).
- [9] S. H. Mazharimousavi, M. Halilsoy, and Z. Amirabi, Phys. Rev. D 81, 104002 (2010);
Classical Quantum Gravity 28, 025004 (2011);
M. R. Mehdizadeh, M. K. Zangeneh, F. S. N. Lobo, Phys. Rev. D 92, 044022 (2015).
- [10] T. Harko, F. S. N. Lobo, M. K. Mak and S. V. Sushkov, Modified-gravity wormholes
without exotic matter, Phys. Rev. D 87, 067504, 1-5, (2013).
- [11] M. G. Richarte and C. Simeone, Thin-shell wormholes supported by ordinary matter in
Einstein-Gauss-Bonnet gravity, Phys. Rev. D 76, 087502 (2007).

- [12] S. O. Alexeyeva, K. A. Rannua, and D. V. Gareevab, Possible Observational Manifestations of Wormholes in the BransDicke Theory, *Journal of Experimental and Theoretical Physics*, Vol. 113, No. 4, pp. 628636, (2011).
- [13] A. DeBenedictis and D. Horvat, On wormhole throats in $f(R)$ gravity theory, *General Relativity and Gravitation* volume 44, pages27112744 (2012).
- [14] M. R. Mehdizadeh and F. S. N. Lobo, Novel third-order Lovelock wormhole solutions, *Phys. Rev. D*, 93, 124014 Published 7 June (2016).
- [15] R. Shaikh and S. Kar, Wormholes, the weak energy condition, and scalar-tensor gravity, *Phys. Rev. D*, 94, 024011 (2016).
- [16] M. R. Mehdizadeh and A. H. Ziaie, Charged wormhole solutions in Einstein-Cartan gravity, *Phys. Rev. D* 99, 064033 Published 22 March (2019).
- [17] M. R. Mehdizadeh and A. H. Ziaie, Charged wormhole solutions in Einstein-Cartan gravity, *Phys. Rev. D* 99, 064033 Published 22 March (2019).
- [18] Buchadahl, H. A., *Mon. Not. Roy. Astron. Soc.* 150, 1 (1970).
- [19] P. Pavlovic, M. Sossich, Wormholes in viable $f(R)$ modified theories of gravity and weak energy condition, *The European Physical Journal C*, **75**, (2015).
- [20] S. Capozziello, M. D. Laurentis, S. D. Odintsov and A. Stabile, Hydrostatic equilibrium and stellar structure in $f(R)$ gravity, *Phys. Rev. D*, 83, 064004 (2011).
- [21] E. Bakirova and V. Folomeev, Dipole magnetic field of neutron stars in $f(R)$ gravity, *General Relativity and Gravitation*, 48, (2016).
- [22] N. R. Napolitano, S. Capozziello, A. J. Romanowsky, M. Capaccioli and C. Tortora, Testing Yukawa-like potentials from $f(R)$ -gravity in elliptical galaxies, *The Astrophysical Journal*, 748, (2012).
- [23] A. Terukina, L. Lombriser, K. Yamamoto, D. Bacon, K. Koyama, R. C. Nichol, Testing chameleon gravity with the Coma cluster, *Cosmology and Nongalactic Astrophysics*, 2014, (2014).
- [24] J. Q. Guo, A. V. Frolov, Cosmological dynamics in $f(R)$ gravity, *Cosmology and Nongalactic Astrophysics*, *Phys. Rev. D*, 88, (2013).
- [25] Planck Collaboration. Planck Results. XIV. Dark energy and modified gravity. *Astronomy and Astrophysics*, 594, (2015).

- [26] C. Arnold, E. Puchwein and V. Springel, The Lyman forest in $f(R)$ modified gravity, Monthly Notices of the Royal Astronomical Society, 448, (2015).
- [27] J. Y. Cen, S. Y. Chien, C. Q. Geng and C. C. Lee, Cosmological evolutions in Tsujikawa model of $f(R)$ Gravity, Physics of the Dark Universe, 26, (2019).
- [28] F. S. N. Lobo and M. A. Oliveira, Wormhole geometries in $f(R)$ modified theories of gravity, Phys. Rev. D, 80, (2009).
- [29] E. F. Eiroa, G. F. Aguirre, Thin-shell wormholes with charge in $F(R)$ gravity, The European Physical Journal C, 76, (2016).
- [30] H. Golchin and M. R. Mehdizadeh, Quasi-cosmological Traversable Wormholes in $f(R)$ Gravity, The European Physical Journal C volume 79, (2019)
- [31] A. K. Mishra, U. K. Sharma, A new shape function for wormholes in $f(R)$ gravity and general relativity, New Astronomy, 88, (2021)
- [32] N. Godania, G. C. Samanta, Traversable wormholes in $f(R)$ gravity with constant and variable redshift functions, New Astronomy 80 (2020).
- [33] K. A. Bronnikov, M. V. Skvortsova and A. A. Starobinsky, Grav. Cosmol. **16**, 216-222 (2010) doi:10.1134/S0202289310030047
- [34] A.D. Felice and S. Tsujikawa “ $f(R)$ Theories,”
- [35] L. Amendola and S. Tsujikawa, Dark Energy: Theory and Observation, Cambridge University Press, (2010)
- [36] K. A. Bronnikov and A. A. Starobinsky, Mod. Phys. Lett. A **24**, 1559-1564 (2009) doi:10.1142/S0217732309030928
- [37] A. D. Dolgov and M. Kawasaki, Can modified gravity explain accelerated cosmic expansion?, Phys. Lett. B 573, 1 (2003).
- [38] R. Bean, D. Bernat, L. Pogosian, A. Silvestri, and M. Trodden, Dynamics of linear perturbations in $f(R)$ gravity, Phys. Rev. D 75 (2007), 064020.
- [39] A. A. Starobinsky, JETP Lett. **86**, 157 (2007).
- [40] B. Bahamonde, M. Jamil, P. Pavlovic and Marko Sossich Phys. Rev. D 94, (2016).

- [41] F. S. N. Lobo and M. A. Oliveira, “Wormhole geometries in $f(R)$ modified theories of gravity,” *Phys. Rev. D* **80**, 104012 (2009)
- [42] S. W. Hawking and G. F. R. Ellis Cambridge University Press, (1973).
- [43] G. Cognola, E. Elizalde, S. Nojiri, S. D. Odintsov, L. Sebastiani and S. Zerbini, “A Class of viable modified $f(R)$ gravities describing inflation and the onset of accelerated expansion,” *Phys. Rev. D* **77**, 046009 (2008)
“Non-singular exponential gravity: a simple theory for early- and late-time accelerated expansion,” *Phys. Rev. D* **83**, 086006 (2011)
- [44] E. Elizalde, S. Nojiri, S. D. Odintsov, L. Sebastiani and S. Zerbini,
- [45] S. Tsujikawa, *Phys. Rev. D* **77**, 023507 (2008) [arXiv:0709.1391 [astro-ph]].
- [46] W. Hu and I. Sawicki, *Phys. Rev. D* **76**, 064004 (2007).
- [47] C. C. Lee, C. Q. Geng and L. yang, Singularity phenomena in viable $f(R)$ gravity, *Progress of Theoretical Physics*, Volume 128, 415-427 (2012).
- [48] C. Q. Geng, Y. T. Hsu and J. R. Lu, Cosmological Constraints on Non-flat Exponential $f(R)$ Gravity, *The Astrophysical Journal* 926, 74 (2022).
- [49] S. Capozziello, V. F. Cardone and A. Troisi, Low surface brightness galaxies rotation curves in the low energy limit of R^n gravity : no need for dark matter?, *Mon.Not.Roy.Astron.Soc*, 375, (2007).
- [50] A. Ali, R. Gannouji, M. Sami, and A. A. Sen, Background cosmological dynamics in $f(R)$ gravity and observational constraints, *Phys. Rev. D* 81, 104029 (2010)
- [51] W. Rindler, *Relativity, Special, General and Cosmology* (Oxford University Press, New York, 2001).
- [52] S. Weinberg, *Gravitation and cosmology: principles and applications of the general theory of relativity*, Wiley (1972).
- [53] K. A. Bronnikov and A. A. Starobinsky, *JETP Lett.* **85**, 1-5 (2007)
doi:10.1134/S0021364007010018